Lack of Neuropathy-Related Phenotypes in *Hint1* Knockout Mice

Kevin L. Seburn, PhD[1], **Kathryn H. Morelli, BS**[1,2], **Albena Jordanova, PhD**[3,4], and **Robert W. Burgess, PhD**[1,2,*]

[1]The Jackson Laboratory, Bar Harbor, Maine.

[2]Graduate School of Biomedical Sciences and Engineering, University of Maine, Orono, Maine.

[3]VIB Department of Molecular Genetics, University of Antwerp, Antwerp, Belgium.

[4]Neurogenetics Laboratory, Institute Born-Bunge, University of Antwerp, Antwerp, Belgium.

Abstract

Mutations in *HINT1*, the gene encoding histidine triad nucleotide-binding protein 1 (HINT1), cause a recessively inherited peripheral neuropathy that involves primarily motor dysfunction and is usually associated with neuromyotonia, i.e. prolonged muscle contraction resulting from hyperexcitability of the peripheral nerve. Because these mutations are hypothesized to cause loss of function, we analyzed *Hint1* knockout mice for their relevance as a disease model. Mice lacking *Hint1* were normal in appearance and in behavioral tests or motor performance, although they moved slower and for a smaller fraction of time than wild-type (WT) mice in an open field arena. Muscles, neuromuscular junctions, and nodes of Ranvier are anatomically normal and did not show evidence of degeneration or regeneration. Axon numbers and myelination in peripheral nerves were normal at 4 and 13 months of age. Axons were slightly smaller than those in WT mice at 4 months of age, but this did not cause a decrease in conduction velocity, and no differences in axon diameters were detected at 13 months. Using electromyography, we were unable to detect neuromyotonia, even using supra-physiological stimuli and stressors such as reduced temperature or 3,4 diaminopyridine to block potassium channels. Therefore, we conclude that *Hint1* knockout mice may be useful for studying the biochemical activities of HINT1, but these mice do not provide a disease model or a means for investigating the basis of HINT1-associated neuropathy and neuromyotonia.

Keywords

Animal model; Axon degeneration; Charcot-Marie-Tooth disease; Histidine triad nucleotide-binding protein 1; *HINT1*; Neuromyotonia

INTRODUCTION

Neuromyotonia is defined as persistent muscle contraction following voluntary movement, resulting from hyperexcitability of the peripheral nerve and not the muscle itself.

Send correspondence and reprint requests to: Robert W. Burgess, The Jackson Laboratory, 600 Main St., Bar Harbor, ME 04609. Phone: 207-288-6706; Fax: 207-288-6077; Robert.burgess@jax.org.

Neuromyotonia can be acquired and is often associated with autoimmune reactivity against voltage-gated potassium channels (1). Peripheral nerve hyperexcitability and myokymia are also found in a number of genetic conditions, including those due to mutations in *KCNA1*, which encodes a potassium channel (1, 2). Recently, mutations in *HINT1*, the gene that encodes histidine triad nucleotide binding protein-1 (HIN1), were identified as causing recessive peripheral neuropathy with neuromyotonia (3). In total, 8 mutations were identified in 33 families, often in a compound heterozygous state although the R37P allele was prevalent and did appear as a homozygous variant. Several lines of evidence suggest that *HINT1* mutations result in a loss of function, including the recessive nature of the disease, the predicted impact of the mutations (including alleles such as Q62*) reduced or eliminated HINT1 protein in patient lymphocytes (genotypes R37P+R37P, R37P+C84R, H51R+C84R, and W123*+W123*) and the inability of those disease-associated variants that do produce stable HINT1 protein to rescue the phenotype of yeast lacking *HNT1*, the yeast ortholog of *HINT1* (3). More recently, a patient with a homozygous H112N variant was also described (4). *HINT1* mutations were also identified in patients with distal hereditary motor neuropathy, a related disorder with distal motor axon degeneration, but without neuromyotonia, indicating clinical variability, but a common theme of predominantly motor involvement (5).

Patients with *HINT1* mutations typically present with neurological symptoms in childhood or early adolescence. A subset of *HINT1* patients has undergone extensive electrophysiological characterization (6). The neuromyotonia can be blocked with curare, thereby establishing that it is neurogenic and not myogenic. It was also present at rest as fasciculations and spontaneous bursts in electromyography (EMG), and was exacerbated by ischemia, low temperature, or voluntary contraction. Hyperexcitability was initiated peripherally, for example, by a blood pressure cuff on the upper arm causing distal neuromyotonia. Thus, the prolonged hyperexcitability is manifest in peripheral axons.

HINT1 is a member of an evolutionarily conserved family of nucleatidyl-transferases and hydrolases. How *HINT1* mutations cause peripheral neuropathy and neuromyotonia is unclear. HINT1 is implicated as a tumor suppressor; consistent with that, haplo-insufficiency results in increased tumor incidence (7, 8). HINT1 also interacts with intracellular signaling pathways, such as regulation of store-operated calcium levels and a direct interaction with Microphthalmia-associated transcription factor (MITF) (9, 10). The HINT1-MITF interaction is regulated by diadenosine tetraphosphate (AP4A), which is produced as a side reaction of tRNA synthetases, and HINT1 enzymatic activity may influence AP4A levels, thereby providing a mechanism for self-regulation (11). Furthermore, mutations in several tRNA synthetase genes (GARS, YARS, AARS, and possibly others) also lead to peripheral neuropathy in humans and mice (Gars), suggesting possible connections between HINT1 activity and peripheral axon degeneration (12–15).

In an attempt to validate *Hint1* knockout mice as a mammalian experimental model system to explore the mechanism through which *HINT1* mutations cause peripheral neuropathy and neuromyotonia, we have thoroughly examined previously existing *Hint1* knockout mice for relevant neurological phenotypes (7). *Hint1* mutant animals were examined for neuromuscular behaviors, nerve, muscle, and neuromuscular junction (NMJ) anatomy, and

electrophysiological analyses of nerve conduction and electromyography. Mice were aged to greater than 1 year and subjected to stressors including low temperature and the potassium channel blocking agent, 3,4 diaminopyridine (3,4 DAP). The mutant mice did not show evidence of axon degeneration or neuromyotonia in any of the tests used under any conditions. Thus, alternative approaches to studying *HINT1*-associated neuropathy need to be devised.

MATERIALS AND METHODS

Mice

Hint1 knockout mice were recovered from cryopreservation at The Jackson Laboratory. These mice were previously generated by deleting exon 1 of *Hint1* in a 129 embryonic stem cell line using standard homologous recombination (7). The strain is on a mixed C57BL/6.129 genetic background, as indicated in the original paper and as confirmed by genetic quality control upon importation to Jackson. Frozen sperm from *Hint1* mutant animals was used in an in vitro fertilization in which C57BL/6J oocyte donors were used. Mice were subsequently maintained by heterozygous intercrossing of the colony to produce the homozygous mutant mice and wild-type (WT) type littermates controls used in the experiments described below. Mice were genotyped by PCR using the following primer combinations: Common Reverse – CGC CCC AFT TAG TTA GTC AG; WT Forward – GCC CCC TGT AAA GTG CAG AC; Mutant Forward – GCC TGA AGA ACG AGA TCA GC. Genomic DNA was prepared from tail-tip or toe-tip biopsy by standard methods and amplified for 40 cycles with a 62°C annealing temperature. Mice were housed under standard vivarium conditions and provided food and water ad libitum. All animal procedures were performed in compliance with the Guide to the Care and Use of Laboratory Animals and were approved by the Institutional Animal Care and Use Committee of The Jackson Laboratory.

Motor Behavior Assays

Mice were tested sequentially on separate days for each of 3 tests of coordinated motor behavior. An equal number of mice of each sex were initially selected for both WT and mutant genotypes, although not all mice successfully completed each task to produce usable data. Animal numbers for each analysis are indicated in the legends. Mice were housed overnight in the room where each test was performed to allow some acclimation and were otherwise housed in similar conditions.

For the Rotarod test, mice were placed on the accelerating (0.1 rpm/s) rotarod (Columbus Instruments, Columbus, OH) for 4 trials separated by 10 minutes. If mice were observed to jump off, turn around, rear, or hang while on the rod they were given an additional attempt for that trial (up to a maximum of 3 for any given trial). Once mice were in position, facing the correct direction, the device was turned on, and mice were required to walk until they lost balance and fell off. The latency (seconds) to a fall was recorded for the successful trial within each round.

Parallel Rod

For the obstacle test, we used a device consisting of a 20-cm-square chamber with clear Plexiglas walls and a floor comprised of stainless steel metal rods with a small space underneath (Clever Sys Inc., Reston, VA). If the animal's foot slipped between the bars into the space below, it was counted automatically by the associated software and stored on computer. In addition, animals were monitored continuously by video so that trials could be reviewed and data validated as necessary. The distance covered was also calculated from the recorded video and allows for the number of foot slips to be normalized to the distance covered.

For the treadmill gait analysis, mice were placed in a Plexiglas enclosure over a treadmill and required to walk at a fixed speed (16.7 cm/sec). Each mouse walked for approximately 30 seconds. A digital video camera, mounted below the clear tread, captured the footfalls of the mouse as they walked for later analysis using specialized software (Treadscan, Clever Sys, Inc.), which generated standard timing and placement measures of the gait phases for each foot/limb. Methods are described in detail elsewhere (16, 17).

For analysis of open field behavior, mice were tested in a dedicated room approximately 1 week after the completion of motor behavior assays. The animals were placed in the arena (60 cm × 60 cm) and their behavior was recorded for 10 minutes. Distance covered and time spent in different areas of the arena were calculated and compared.

EMG recordings for detection of neuromyotonia

Mice were anesthetized with isoflurane and EMGs were recorded from muscles in the foot in response to proximal stimulation of the sciatic nerve at the level of the sciatic notch. Initial attempts were made in 4 mutant animals at 4 months of age using 6 10-pulse trains delivered every 2 seconds at normal physiological temperature at frequencies of both 50 and 100 Hz. Each individual record was examined for non-evoked EMG activity both between pulses and for 1.5 seconds after the last pulse.

A second set of experiments was then conducted on 4 additional mutants to evaluate age, cold stress and K^+ channel blockade. The same stimulation protocols were repeated in older mice (4.5, 7 and 13 months of age; n = 1, 2 and 1, respectively) at rectal temperatures of 37°, 35°, 33° and 31°C. A final set of records was then collected with the same stimulus protocol beginning 30 minutes after mice had been administered 3,4 DAP (5 mg/kg) at 37°, 35°, 33°, and 31°C. To avoid the concern that our stimulus may have been insufficient, we recorded from 2 additional 13-month-old mutant mice using a much longer stimulus train (1.5 sec at 100 Hz); both at reduced temperatures and 30 minutes after administration of 3,4 DAP.

Finally, we examined an additional muscle using an alternative anesthetic. In 2 8-month-old mutant mice (1 male, 1 female), anesthetized with intraperitoneal 2% tribromoethanol (Avertin, 400 mg/kg), we again used the supra-physiological stimulus train (1.5 seconds at 100 Hz) and examined EMG recorded from medial gastrocnemius at both 37° and 31°C (rectal temperature).

Histology and immunolabeling

Methods for histology and immunolabeling have been described previously in detail (15, 18, 19). In brief, the entire triceps surae (medial and lateral gastrocnemius, soleus) and plantaris were dissected free from both hind legs, weighed, and 1 muscle was fixed in Bouin's fixative, paraffin-embedded, and sectioned for standard histology with hematoxylin and eosin stain. Muscles were examined by a veterinary pathologist at The Jackson Laboratory. The plantaris of the other leg was fixed for 4 hours in ice-cold buffered 4% paraformaldehyde and used for NMJ staining. NMJ morphology was evaluated blind to genotype following labeling of the acetylcholine receptors with Alexa-594 conjugated α-bungarotoxin (Invitrogen, Carlsbad, CA) and a cocktail of anti-neurofilament (2H3) and anti-SV2 to label the motor axon and terminal (Developmental Studies Hybridoma Bank, Iowa City, IA). Nerves were visualized with an Alexa-488 conjugated anti-mouse IgG1 antibody (Invitrogen).

Femoral nerves were dissected free and fixed by immersion in 2% paraformaldehyde, 2% glutaraldehyde in 0.1 M cacodylate buffer. Nerves were then plastic embedded, sectioned at 0.5-μm thickness, and stained with Toluidine blue. Images were collected at 40× magnification on a Nikon Eclipse 600 microscope with DIC-Nomarski optics. Images were analyzed for axon number and axon diameter using an automated method in Fiji/ImageJ (areas) that was manually verified. The same embedded samples were also sectioned at 75 nm, counterstained by standard methods, and mounted on grids for examination by electron microscopy using a Jeol 1230 electron microscope equipped with a Hamamatsu digital camera system. Myelin compaction was measured at 60,000× magnification by measuring the thickness of myelin and counting the number of wraps contributing to that thickness. Between 3 and 8 measurements were made from each sample.

For immunohistochemistry, sciatic nerves were dissected free, fixed in cold, buffered 2% paraformaldehyde for 45 minutes, and teased onto glass slides in a drop of phosphate-buffered saline. Samples were allowed to dry onto the slides overnight and then extracted in −20°C acetone for 10 minutes. Samples were blocked and permeabilized in phosphate-buffered saline with 1% bovine serum albumin and 0.5% Triton X-100 for 1 hour at room temperature. Primary antibodies were diluted in blocking buffer and applied overnight at 4°C. Following washes, secondary antibodies were also applied overnight at 4°C. The following primary antibodies were used: anti-contactin-associated protein (CASPR)/Neuroexin IV (mouse monoclonal IgG1, NeuroMab/Antibodies Inc., Davis, CA; 1:250 dilution), anti-Kv1.2 (mouse monoclonal IgG2b$_K$, Millipore, Billerica, MA; 1:100 dilution), anti-NaV1.6 (mouse monoclonal IgG1, NeuroMab/Antibodies Inc., 1:5 dilution), anti-NaV1.6 (rabbit, Alamone, Jerusalem, Israel; 1:200 dilution), anti-Ankyrin G (rabbit, Santa Cruz Biotechnology, Santa Cruz, CA; 1:200). The following secondary antibodies (Invitrogen) were used for visualization: anti-mouse IgG1 Alexa 594, anti-mouse IgG1 Alexa 488, anti-mouse IgG2b$_K$ Alexa 488, anti-rabbit Alexa 594, and anti-rabbit Alexa 647.

Statistics

A one-way ANOVA was used for comparison of genotypes for axon counts, conduction velocity, Parallel Rod, Gait and Open field. Rotarod data were analyzed using 2-way

ANOVA (trial by genotype) followed by Tukey's HSD post-hoc comparison. Axon areas, diameters, and G-ratios were compared using the non-parametric Kolmogorov-Smirnov two-sample test. Probability of $p < 0.05$ was used as a cutoff for declaring statistical significance in all comparisons.

RESULTS

Gross motor performance in *Hint1* knockout mice

The *Hint1* knockout mice have been previously characterized for their tumor susceptibility, but they have not been rigorously examined for neuropathy-related phenotypes (7, 8). Mutant mice are reported to be overtly normal, except that males weighed significantly less than littermates between 5 and 7 months of age. No histological or morphological differences were seen in brain, heart, kidney, liver or spleen (7). Consistent with these observations, mutant mice from our colony were overtly normal in appearance and size, although we did not perform a detailed growth curve and body weight beyond 2 months of age, an mutant mice did not show obvious abnormalities in movement or coordination. To assess motor performance rigorously, we used 3 well-established tests: gait analysis, rotarod, and a parallel rod test.

To assess gait, mice were videotaped walking on a clear treadmill, and gait parameters were derived from curated video analysis of footfalls (16, 17). Comparison of the 3 primary gait phases for the rear limbs (stride time, stance time, and swing time) showed no differences (Fig. 1a). Front limb parameters and a variety of other gait measures (e.g. stance width, stride length) were also not different (data not shown). Thus, *Hint1* mutant mice walked normally.

The rotarod test of coordination involves placing mice on a rotating cylinder and recording the latency to falling off. This test depends on a number of factors, including balance (vestibular and cerebellar function), proprioception, and appropriate motor output. Rotarod performance of *Hint1* mice improved over 4 trials (increased latency to fall), demonstrating normal short-term motor learning, and was not different than controls (Fig. 1b). Failed trials occurred at least once for most mice of both genotypes (see Materials and Methods). Thus, *Hint1* knockout mice have normal coordination, motor learning and ability in this test.

In the parallel rod test, mice were placed in a chamber with a floor comprised of evenly spaced metal rods for 10 minutes. The animals were recorded on video for the entire session and then recordings were analyzed for ambulation and "errors." The total distance travelled was similar for both genotypes (204 ± 10 vs. 211 ± 5 cm for *Hint1* mutant and WT, respectively), as was the number and duration of foot slips (Fig. 1c). Thus, *Hint1* mutant mice also showed no motor deficits in this test.

Hint1 mice are less active and move more slowly in Open Field test but show no differences in anxiety-related behaviors

The gait and rotarod tests require mice to move at a pace set by the experimenter. To assess mice moving of their own volition on a regular surface, we used an open field apparatus. In this test, *Hint1* mutant animals moved less and moved more slowly than control mice. The

total distance travelled by *Hint1* mutant mice was approximately half that covered by WT controls (Fig. 2a). The difference was the result of both a decrease in the speed of movement and the percentage of time the mutant mice spent moving (Fig. 2b, c). The open field is also used to assess anxiety, with anxious mice spending more time near the wall of the apparatus and less time in the center. Furthermore, anxious mice tend to freeze, possibly contributing to the differences observed. *Hint1* mutant mice are reported to have anxiety-like phenotypes, although male mice in an open field reportedly did not show differences in anxiety measures or total distance traveled (20). In our experiments there was no difference between genotypes in the proportion of time spent in different areas of the arena (center vs. perimeter) or in amount of rearing, urination or defecation (data not shown), suggesting that the mutant mice were not more anxious than controls. Thus, freely moving *Hint1* mutant mice moved less and more slowly than control mice, but the reason for this behavioral difference is unclear.

Peripheral muscle and nerve analysis

The *Hint1* mutant mice did not show deficits in motor performance beyond reduced speed and activity in an open field; however, we also wanted to investigate possible anatomical changes that would not necessarily manifest themselves in behavior tests. As a first assessment, paraffin sections of the triceps surae of 6 mutant and 4 WT littermate control mice between 7 and 13 months of age were cross-sectioned and stained with hematoxylin and eosin (7 months, 1 mutant, 1 WT male, 1 mutant female; 13 months, 1 mutant, 2 WT males, 3 mutant and 1 WT females). No evidence of fibrosis, atrophy, or regeneration was observed (data not shown), and ratios of muscle weight to body weight, an indicator of selective muscle atrophy or hypertrophy, were also normal (9.2 ± 2.2 mg/g for *Hint1* mutants vs. 10.4 ± 0.6 mg/g for control mice, p = 0.3). We also examined NMJs of the plantaris muscle of the same mice using a cocktail of antibodies against motor axons and terminals and α-bungarotoxin to label postsynaptic acetylcholine receptors. The overall morphology of NMJs was normal, with a complex pretzel-like shape and no signs of fragmentation, presynaptic sprouting, or other indicators of degeneration (Fig. 3A, B). The motor nerve terminal fully overlapped the postsynaptic receptors to an extent comparable to the controls (97 ± 1% of junctions fully occupied in mutant samples vs. 95 ± 2% in controls). Therefore, there was no indication of a synaptic defect in *Hint1* mutant muscles.

We also examined nodes of Ranvier in teased axons from the sciatic nerves of the same 7-13-month-old animals. Nodes double-labeled with antibodies against NaV1.6 sodium channels, the primary sodium channel at adult peripheral nodes, and Ankyrin G, an intracellular scaffolding protein necessary for NaV1.6 localization, were independently examined by 2 investigators blinded to genotype. No discernable differences in localization, alignment, or morphology of these proteins were found. Given the hyperexcitability of peripheral axons associated with neuromyotonia, the examination of potassium channels may also be a directly relevant phenotype. Therefore, we also labeled nodes with additional antibodies to the paranode (anti-CASPR) and the juxtaparanode (anti-KV1.2) (Fig. 3C, D). No changes in the alignment or morphology of the nodal Ankyrin G, paranodal CASPR or juxtaparanodal KV1.2 channels were observed.

The numbers and sizes of peripheral axons were examined at 3 to 4 months and 13 months in the femoral nerve, which consists of a primarily motor branch innervating the quadriceps and a primarily sensory branch that becomes the saphenous nerve innervating the skin of the lower leg. Peripheral nerves in cross-section had normal axonal and myelin anatomy (Fig. 3 E, F). At 3 to 4 months of age, numbers of axons in the motor branch of the femoral nerve were not different between mutant and littermate control animals (Fig. 4a). In addition, the distributions of axon areas were also very similar. The cross-sectional areas of individual axons (excluding myelin) in the motor branch of the femoral nerve were determined using semi-automated image analysis. The distribution of these axon areas for mutant and control samples is shown as a cumulative histogram, in which the percent of the total sample (Y axis) is plotted against the area of individual axons (X axis) (Fig. 4b). Although the shape of the distributions was very slightly, but significantly different (Kolmogorov-Smirnov, $p < 0.001$), compared to other neuropathy models, this is not a major effect (15, 21). Moreover, peripheral nerve function, assessed with measurement of nerve conduction velocities, was not different between mutant and control animals (Fig. 4c).

To examine the possible appearance of neuropathy with age, we also performed nerve morphometry on 4 mutant and 3 control samples from 13-month-old mice. The number of axons did not differ between genotypes at 13 months (568 ± 21 WT vs. 553 ± 32 mutant, $p = 0.5$). Inner (axonal) and outer (axon plus myelin) fiber diameters were measured and G-ratios (inner/outer) were calculated. No differences were found in the distribution of axon diameters or G-ratios (Fig. 4d, e), or the relationship between G-ratio and axon diameter (Fig. 4f). These measures suggest that both axons and myelin are intact in mutant mice at over 1 year of age. To confirm this further, these samples were also viewed using electron microscopy and no consistent differences between mutant and control samples were found. Myelin compaction was also measured at 60,000× magnification and found to be equivalent between mutant and controls (14.7 ± 0.6 nm/wrap in WT, 14.1 ± 0.6 nm/wrap in mutants, $p = 0.25$, t-test). These results are consistent with the similar axon size, myelination, and nodal and NMJ anatomy. Quantification was done on the motor branch of the femoral nerve, given the predominantly motor deficits in *HINT1* patients; however, sensory nerves were also examined and did not show obvious phenotypes at either age (data not shown).

Hint1 mutant mice do not show neuromyotonia

There were no overt signs of neuromyotonia observed in mice while in their home cages or in behavioral tests of motor performance. To test for the presence of neuromyotonia, we monitored and recorded EMGs in the foot muscles during proximal stimulation of the sciatic nerve in anesthetized mutant mice. We attempted to evoke neuromyotonia in mice of different ages under several different conditions and stimulus protocols (Methods and data not shown). In Fig. 5, we show data from a 13-month-old mutant mouse in response to a 1.5-second, 100 Hz stimulus train. A complete record taken at normal body temperature (37°C) showed no evidence of neuromyotonia (Fig. 5a). This stimulus protocol was repeated with body temperature lowered to 31°C and in the presence of 3,4 diaminopyridine, a potassium channel antagonist. Both conditions affected nerve conduction, as shown by comparison of the first compound muscle action potential (CMAP) response under each condition (Fig. 5b, c). However, there was no evidence of neuromyotonia either between pulses or after the

entire stimulus train in any of the tested conditions, as shown in the traces of the final 4 CMAP responses from the train (Fig. 5d).

Two additional 8-month-old mutant mice (1 male, 1 female) were tested for neuromyotonia using tribromoethanol (Avertin) instead of isoflurane anesthesia to ensure that the hyperexcitability was not being masked by the anesthetic. In addition, in these mice, EMG recordings were made from the gastrocnemius to increase the chance of seeing abnormal motor unit firing. These mice were subjected to the same supra-physiological 1.5-second, 100 Hz stimuli at body temperatures from 37° to 31°C. This procedure, examining a different, larger muscle under Avertin anesthesia, also failed to elicit abnormal EMG activity that would indicate neuromyotonia. In previous studies, an equivalent experimental preparation revealed abnormal, delayed, asynchronous EMG activity in $Lama2^{dy/dy}$ mutant mice at much lower stimulus intensities (not shown), indicating that our recordings should be sensitive enough to detect such activity if it had arisen.

DISCUSSION

The $Hint1$ knockout mice show no indication of peripheral neuropathy or neuromyotonia up to 14 weeks of age, or under any condition tested. We feel there are 3 possible explanations for this, which are discussed below.

First, our analyses may have failed to detect the phenotype. We do not favor this explanation given the combination of approaches used (behavioral, anatomical, and electrophysiological) and the conditions tested (ages to >1 year, low temperature, K^+ channels blockers, and a variety of stimulation protocols including supra-physiological conditions). The analyses used here are generally sensitive enough to detect changes in other peripheral neuropathy and neuromuscular disease models (15, 19, 21). However, there are caveats to our analysis. We do not have a good positive control for measuring myotonia, although we should have found any associated peripheral axon degeneration or atrophy. We also had to perform our electrophysiological analyses under anesthesia (isoflurane or tribromoethanol), which may affect excitability. Mice are susceptible to neuromyotonia in demyelinating neuropathy models (22–24), and we have previously recorded abnormal EMG activity and observed myokymic twitches, both of which were readily detected even under anesthesia in $Lama2$ mutant mice, which have hypomyelination and are a model of congenital muscular dystrophy type 1A (25). Thus, the hyperexcitability caused by loss of $Hint1$ would have to be subtler and more sensitive to anesthesia than other models.

Electrical stimulation in human patients with hereditary motor neuropathy failed to evoke neuromyotonia, whereas voluntary contraction did (6). We had to use electrical stimulation to examine peripheral nerve properties in anesthetized animals. However, we used a variety of electrical stimuli including conditions that are more extreme than those used clinically (e.g. 100 Hz, 1.5 seconds), and in combination with cold and K^+ channel blockade, yet we still failed to elicit neuromyotonia. Again, this should not have masked our ability to detect peripheral axon loss or atrophy, and our behavioral assessments, including treadmill walking, rotarod, and parallel rod test, require voluntary muscle contraction, but also failed to show differences in mutant animals.

A second possibility is that mice are not susceptible to *Hint1*-associated neuropathy and neuromyotonia. This may be for neurophysiological or biochemical reasons. The neurophysiological basis of neuromyotonia and its relationship to peripheral neuropathy are unclear; however, involvement of potassium channels as the normal driving force of membrane repolarization and refractory periods is plausible. Indeed, mice show neuromyotonia with a similar profile to that described in *HINT1* patients when Kv1.1 potassium channels are mutated, or in acquired immune-mediated neuromyotonia (26, 27). In addition to the demyelinating mouse mutations mentioned above, mice also show neuromyotonia when acetyl cholinesterase at the NMJ is compromised by reduced levels of perlecan (28, 29). Thus, mouse neurophysiology can manifest neuromyotonia under conditions consistent with hyperexcitability (e.g. decreased potassium channel activity or decreased acetylcholineesterase), and we would have to invoke special circumstances regarding the *Hint1* neuromyotonia that make mice less susceptible.

Biochemically, mice may be better able to compensate for the loss of *Hint1* than humans, either through greater redundancy or differences in biochemical pathways. Such compensation may be challenging to detect because it may be neuron-specific and because the full range of HINT1 substrates and activities are unknown. The intracellular associations of HINT1 are regulated by levels of AP4P, produced as a side reaction of tRNA synthetases. The primary function of tRNA synthetases is to charge amino acids onto their cognate tRNAs for translation. This is a two-step reaction, in which ATP and the amino acid bind, producing an aminoacyl adenylate (aaAMP) intermediate and pyrophosphate. The aaAMP is then used to bind the amino acid to the 3' end of the tRNA. Several tRNA synthetases are able to combine aaAMP with ATP, to produce AP4A. HINT1 has been shown to hydrolyze Lysine-AMP and other aaAMPs, thus possibly impacting AP4A levels and, therefore, HINT1's own interactions with partners such as MITF (30). An examination of AP4A or aaAMP levels in *Hint1* knockout mice may be interesting but even if changes were found, it is unknown if these metabolites are part of the neuropathy disease mechanism or related to other aspects of HINT1 biology, such as tumor suppression. Differences in substrate preferences have been reported for HINT1 from different species (31). As HINT1 biochemistry is further examined, it will be interesting to determine if there are changes in substrate preference, kinetics, or other activities between the human and mouse proteins that may suggest why loss of HINT1 only causes neuropathy in people.

A third possible explanation is that the human phenotype may not be the result of a straight loss-of-function. The mice used in the present study carry a deletion of the first exon of *Hint1*, and have been shown to be null, with no detectable protein produced (7). In humans, seemingly unambiguous loss-of-function alleles such as Q62* were identified, and other variants such as R37P appear to be very unstable and are degraded in yeast and human cells ([1] and Albena Jordanova, unpublished observations). Furthermore, the recessive nature of the disease is consistent with a loss-of-function. However, this may instead reflect a requirement for reduced WT protein to see a pathological effect of mutant gain-of-function alleles. Because the protein normally forms a homodimer, the presence of WT protein in heterozygous genotypes may prevent the mutant forms from mislocalizing or otherwise acting detrimentally. Thus, a complete loss of HINT1 may be less damaging than a

pathological gain-of-function mutant allele, either as a homozygote or in combination with a null allele, but in the absence of WT. Analysis of additional *HINT1* patients carrying new alleles may resolve this question, or human mutations such as C84R or W123*, which produce detectable mutant proteins, could be introduced into the mouse gene. Both residues are conserved and could be studied as homozygotes, compound heterozygotes, or in combination with the null knock out allele examined here.

Therefore, we suggest the following possibilities to generate a *HINT1* neuropathy/neuromyotonia disease model: The knockout mouse mutation could be moved to other genetic backgrounds (presently, the mice carry a mixed 129/C57BL/6 background) to determine whether a different combination of background loci may create a more sensitive genotype. Indeed, even the yeast phenotypes of sensitivity to carbon source and temperature are not completely penetrant across all yeast strains ([31] and Albena Jordanova, unpublished observations). Given the compelling evidence for a loss of function in humans, the background influence seems like the most plausible issue in mice. In addition, specific human alleles, particularly those that produce stable protein variants, could be introduced into the mouse genome. Alternatively, a different model organism such as rats or zebra fish may more successfully recapitulate the human disease. More sensitive neurophysiological and electromyographic methods, particularly if they allow analysis in awake, voluntarily behaving animals, may reveal phenotypes that are currently hidden by the requirement for anesthesia and electrical stimulation of nerves. The *Hint1* mutant mice do, however, provide a system for biochemical and metabolic analysis of HINT1 activity; such analyses should be performed in parallel with examination of the human enzyme or patient cell lines to determine if HINT1 in mice has the same properties as human HINT1.

Our results are of value because they demonstrate that the absence of HINT1 does not necessarily lead to neuropathy and neuromyotonia in mammals. However, we have failed to establish *Hint1* knockout mice as a useful disease model. Investigators interested in pursuing studies of HINT1 and neurological disease need to consider these findings and explore alternative approaches or analyses to understand how *HINT1* mutations cause neuropathy and neuromyotonia in humans.

Acknowledgments

REFERENCES

1. Maddison P. Neuromyotonia. Clinical Neurophysiol. 2006; 117:2118–2127.

2. Browne DL, Gancher ST, Nutt JG, et al. Episodic ataxia/myokymia syndrome is associated with point mutations in the human potassium channel gene, KCNA1. Nature Gen. 1994; 8:136–140.

3. Zimon M, Baets J, Almeida-Souza L, et al. Loss-of-function mutations in HINT1 cause axonal neuropathy with neuromyotonia. Nature Gen. 2012; 44:1080–1083.

4. Caetano JS, Costa C, Baets J, et al. Autosomal recessive axonal neuropathy with neuromyotonia: a rare entity. Pediatr Neurol. 2014; 50:104–107. [PubMed: 24131582]

5. Zhao H, Race V, Matthijs G, et al. Exome sequencing reveals HINT1 mutations as a cause of distal hereditary motor neuropathy. Eur J Hum Gen. 2013 Oct 9. [Epub ahead of print].

6. Hahn AF, Parkes AW, Bolton CF, et al. Neuromyotonia in hereditary motor neuropathy. J Neurol Neurosurg Psych. 1991; 54:230–235.

7. Su T, Suzui M, Wang L, et al. Deletion of histidine triad nucleotide-binding protein 1/PKC-interacting protein in mice enhances cell growth and carcinogenesis. Proc Natl Acad Sci USA. 2003; 100:7824–7829. [PubMed: 12810953]

8. Li H, Zhang Y, Su T, et al. Hint1 is a haplo-insufficient tumor suppressor in mice. Oncogene. 2006; 25:713–721. [PubMed: 16186798]

9. Razin E, Zhang ZC, Nechushtan H, et al. Suppression of microphthalmia transcriptional activity by its association with protein kinase C-interacting protein 1 in mast cells. J Biol Chem. 1999; 274:34272–34276. [PubMed: 10567402]

10. Linde CI, Feng B, Wang JB, et al. Histidine triad nucleotide-binding protein 1 (HINT1) regulates Ca(2+) signaling in mouse fibroblasts and neuronal cells via store-operated Ca(2+) entry pathway. Am J Physiol. Cell physiology. 2013; 304:C1098–C1104.

11. Goerlich O, Foeckler R, Holler E. Mechanism of synthesis of adenosine(5')tetraphospho(5')adenosine (AppppA) by aminoacyl-tRNA synthetases. Eur J Biochem. 1982; 126:135–42. /FEBS 1982: 126;135-42. [PubMed: 7128581]

12. Antonellis A, Ellsworth RE, Sambuughin N, et al. Glycyl tRNA synthetase mutations in Charcot-Marie-Tooth disease type 2D and distal spinal muscular atrophy type V. Am J Hum Gen. 2003; 72:1293–1299.

13. Jordanova A, Irobi J, Thomas FP, et al. Disrupted function and axonal distribution of mutant tyrosyl-tRNA synthetase in dominant intermediate Charcot-Marie-Tooth neuropathy. Nature genetics. 2006; 38:197–202. [PubMed: 16429158]

14. Latour P, Thauvin-Robinet C, Baudelet-Mery C, et al. A major determinant for binding and aminoacylation of tRNA(Ala) in cytoplasmic alanyl-tRNA synthetase is mutated in dominant axonal Charcot-Marie-Tooth Disease. Am J Hum Gen. 2010; 86:77–82.

15. Seburn KL, Nangle LA, Cox GA, et al. An active dominant mutation of glycyl-tRNA synthetase causes neuropathy in a Charcot-Marie-Tooth 2D mouse model. Neuron. 2006; 51:715–726. [PubMed: 16982418]

16. Wooley CM, Sher RB, Kale A, et al. Gait analysis detects early changes in transgenic SOD1(G93A) mice. Muscle Nerve. 2005; 32:43–50. [PubMed: 15880561]

17. Wooley CM, Xing S, Burgess RW, et al. Age, experience and genetic background influence treadmill walking in mice. Physiology & behavior. 2009; 96:350–361. [PubMed: 19027767]

18. Burgess RW, Cox GA, Seburn KL. Neuromuscular disease models and analysis. Meth Molec Biol. 2010; 602:347–393.

19. Motley WW, Seburn KL, Nawaz MH, et al. Charcot-Marie-Tooth-linked mutant GARS is toxic to peripheral neurons independent of wild-type GARS levels. PLoS Gen. 2011; 7:e1002399.

20. Varadarajulu J, Lebar M, Krishnamoorthy G, et al. Increased anxiety-related behaviour in Hint1 knockout mice. Behavioural brain research. 2011; 220:305–311. [PubMed: 21316396]

21. Achilli F, Bros-Facer V, Williams HP, et al. An ENU-induced mutation in mouse glycyl-tRNA synthetase (GARS) causes peripheral sensory and motor phenotypes creating a model of Charcot-Marie-Tooth type 2D peripheral neuropathy. Dis Mod Mech. 2009; 2:359–373.

22. Toyka KV, Zielasek J, Ricker K, et al. Hereditary neuromyotonia: a mouse model associated with deficiency or increased gene dosage of the PMP22 gene. J Neurol Neurosurg Psych. 1997; 63:812–813.

23. Zielasek J, Toyka KV. Nerve conduction abnormalities and neuromyotonia in genetically engineered mouse models of human hereditary neuropathies. Ann NY Acad Sci. 1999; 883:310–320. [PubMed: 10586256]

24. Zielasek J, Martini R, Suter U, et al. Neuromyotonia in mice with hereditary myelinopathies. Muscle & nerve. 2000; 23:696–701. [PubMed: 10797391]

25. Patton BL, Wang B, Tarumi YS, et al. A single point mutation in the LN domain of LAMA2 causes muscular dystrophy and peripheral amyelination. J Cell Sci. 2008; 121:1593–1604. [PubMed: 18430779]

26. Shillito P, Molenaar PC, Vincent A, et al. Acquired neuromyotonia: evidence for autoantibodies directed against K+ channels of peripheral nerves. Ann Neurol. 1995; 38:714–722. [PubMed: 7486862]

27. Brunetti O, Imbrici P, Botti FM, et al. Kv1.1 knock-in ataxic mice exhibit spontaneous myokymic activity exacerbated by fatigue, ischemia and low temperature. Neurobiol Dis. 2012; 47:310–321. [PubMed: 22609489]

28. Bangratz M, Sarrazin N, Devaux J, et al. A mouse model of Schwartz-Jampel syndrome reveals myelinating Schwann cell dysfunction with persistent axonal depolarization in vitro and distal peripheral nerve hyperexcitability when perlecan is lacking. Am J Pathol. 2012; 180:2040–2055. [PubMed: 22449950]

29. Stum M, Girard E, Bangratz M, et al. Evidence of a dosage effect and a physiological endplate acetylcholinesterase deficiency in the first mouse models mimicking Schwartz-Jampel syndrome neuromyotonia. Human Molec Gen. 2008; 17:3166–3179.

30. Wang J, Fang P, Schimmel P, et al. Side chain independent recognition of aminoacyl adenylates by the Hint1 transcription suppressor. J Phys Chem B. 2012; 116:6798–6805. [PubMed: 22329685]

31. Bieganowski P, Garrison PN, Hodawadekar SC, et al. Adenosine monophosphoramidase activity of Hint and Hnt1 supports function of Kin28, Ccl1, and Tfb3. J Biol Chem. 2002; 277:10852–10860. [PubMed: 11805111]
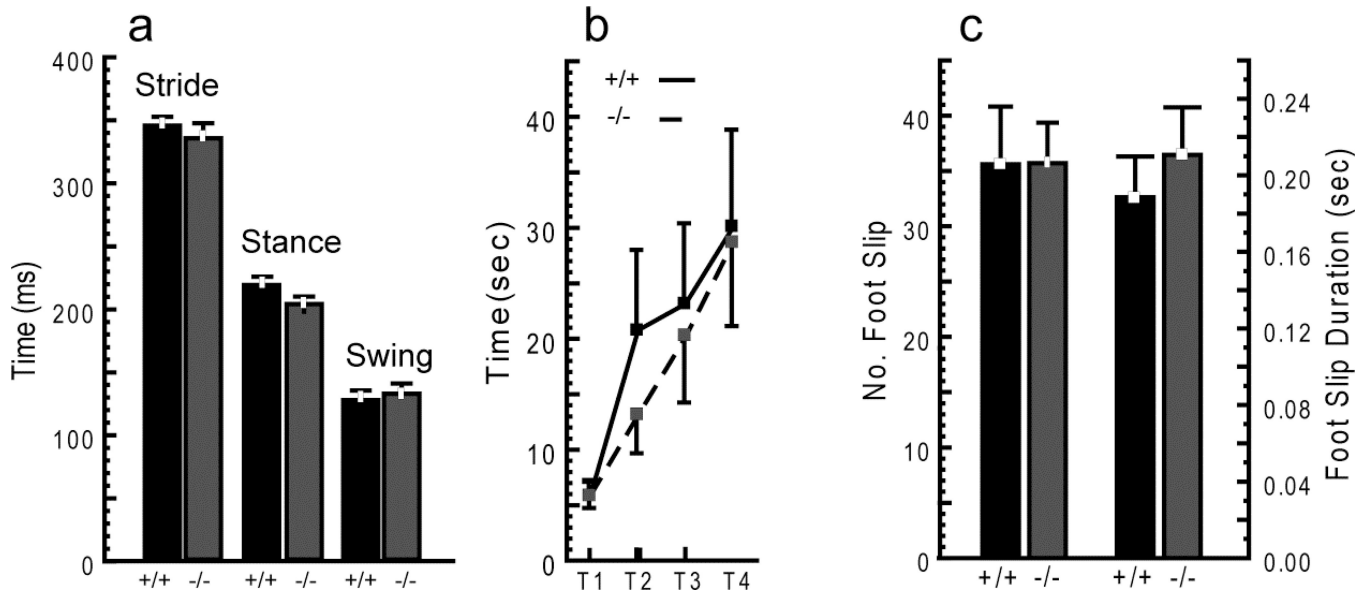
Figure 1.
No detectable differences in motor performance between *Hint1* mutant (−/−) and wild type (WT) (+/+) mice. (**a**) *Hint1* mutant mice have a normal gait pattern. Video analysis of treadmill walking for rear limb stride time, stance time, and swing time showed no differences. (**b**) *Hint1* mutant mice perform as well as WT mice on Rotarod. Performance of both *Hint1* mutant and control mice improved over 4 trials (increased latency to fall). (**c**) *Hint1* mutant mice negotiate parallel rod obstacle equally as well as WT mice with no increase in the number or duration of foot slips. ANOVA, p 0.4 all comparisons in **a–c**. Values are mean ± SE (Gait: n = 12 WT [7 female, 5 male], 10 mutant [7 female, 3 male]; Rotarod: n = 13 WT [7 female, 6 male], 15 mutant [9 female, 6 male]; and parallel rod: n = 13 WT [7 female, 6 male], 14 mutant [9 female, 5 male]). Mice were tested at 88, 92 and 114 days of age on rotarod, parallel rod and gait, respectively.
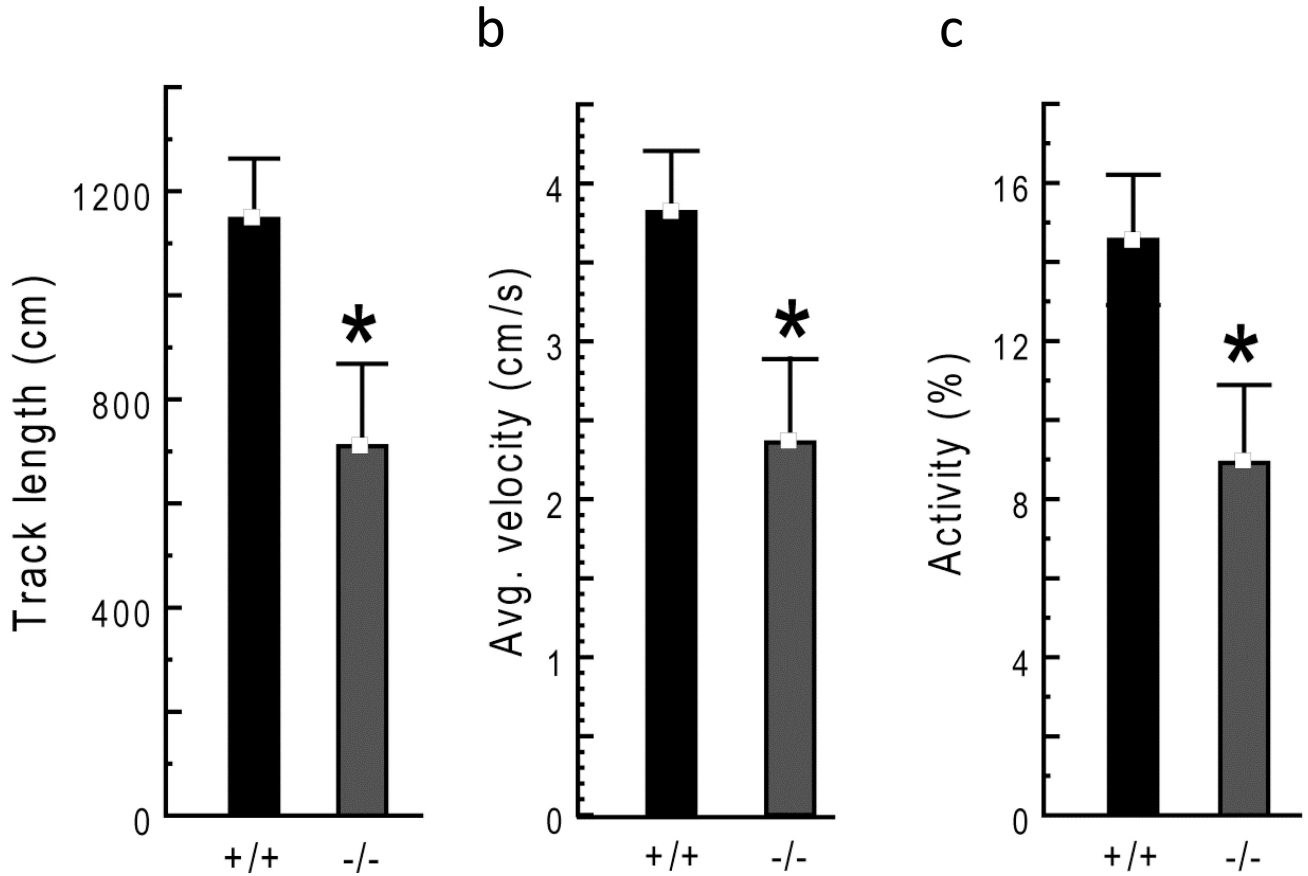
a b c

Figure 2.
Hiat1 mutant mice show decreased movement in the open field test. (**a**) In a 10-minute trial the total distance travelled by *Hint* 1 knockout mice (–/–) was almost halved compared to that covered by wild-type (WT) (+/+) controls. (**b**) The speed of movement of the mutant mice was also significantly slower. (**c**) The percentage of time the mutant mice spent moving was also decreased. ANOVA, p   0.04 all comparisons. Values are mean ± SE (n = 13 WT [7 female, 6 male], 14 mutant [9 female, 5 male], Mice tested between 90 and 120 days of age).
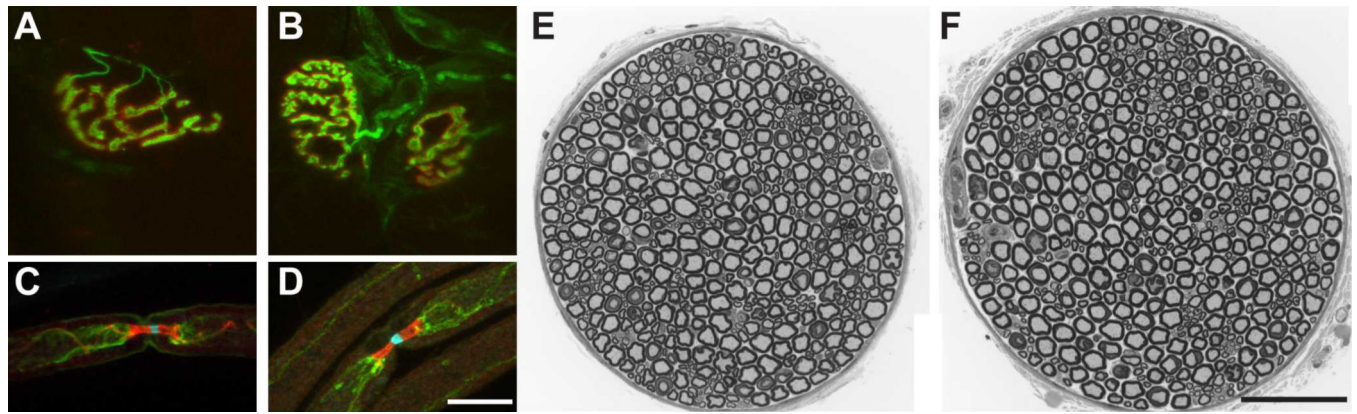
Figure 3.
Neuromuscular junctions (NMJs), node of Ranvier, and peripheral nerve anatomy. (**A, B**) NMJs have normal morphology of motor nerve terminals (green) and postsynaptic end plates (red) in control (**a**) and *Hint1* mutant (**b**) animals. (**C, D**) Nodes of Ranvier are also normal in morphology in control (**C**) and *Hint1* mutant (**D**) mice. Nodes were triple-labeled with antibodies against Ankyrin G (cyan), the paranode with antibodies against contactin-associated protein (CASPR, red), and the juxtaparanode with antibodies against KV1.2 potassium channels (green). (**E, F**) Peripheral nerve morphology also appeared normal in cross-sections of the motor branch of the femoral nerve. NMJs and nodes were examined in 6 mutant mice and 4 littermate controls at 7 to 13 months of age. Femoral nerves were analyzed in the same mice, and in 3 mutant and 3 control mice at 3 months of age. Scale bars: **A–D**, 14 μm; **E, F**, 50 μm.
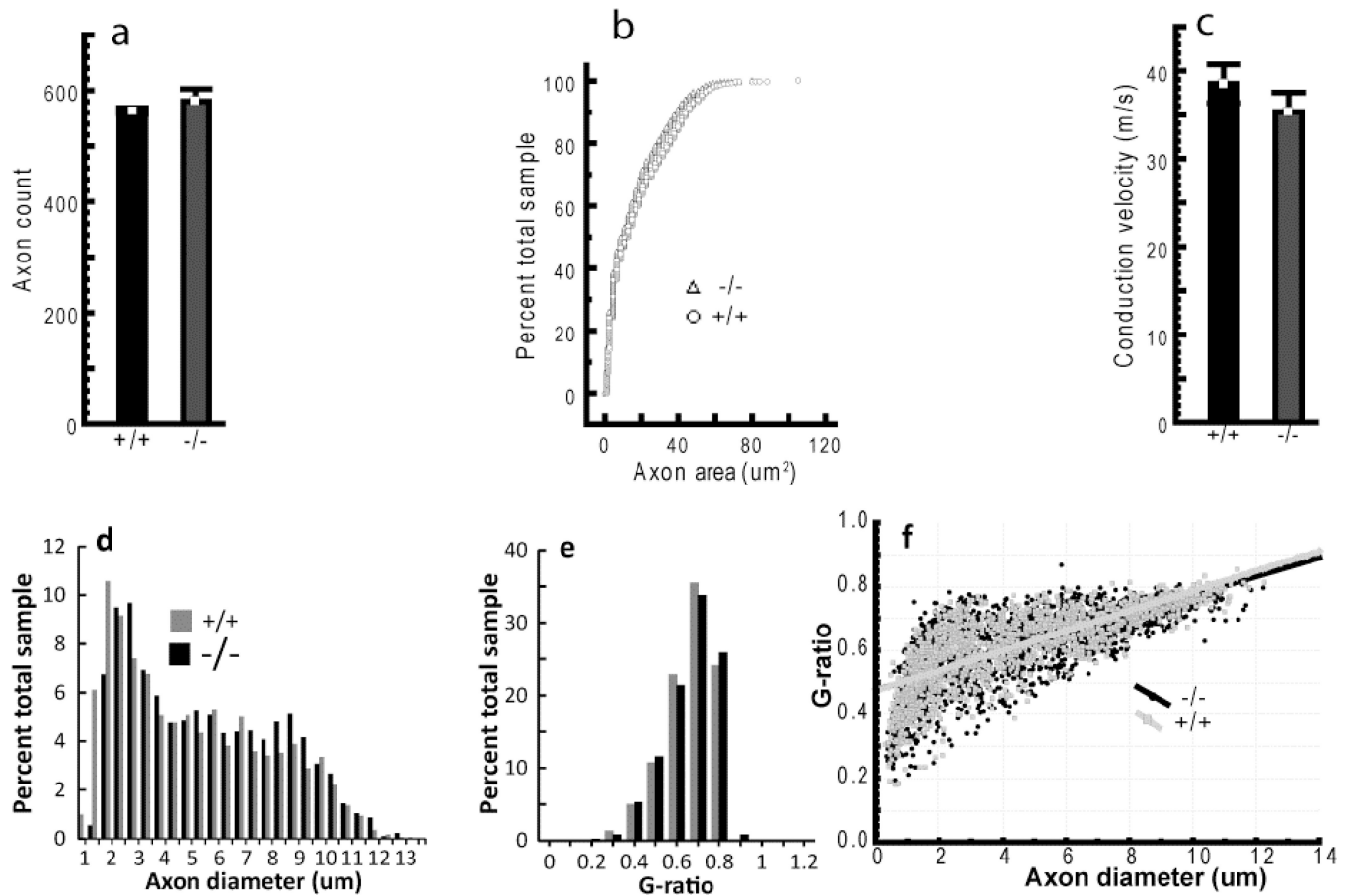
Figure 4.

Number, size and function of axons are unchanged in *Hint1* mutant mice. (**a**) Femoral motor nerve axon counts were not different. (**b**) Similarly, the distribution of axon areas showed almost complete overlap. In the cumulative histogram shown, the percent of the total sample is graphed against the area of individual axons. Although the distributions were statistically different (Kolmogorov-Smirnov, p < 0.001), the small change in the shape of the distribution that was detected was not functionally relevant. Axon counts and areas were measured in 3 animals of each genotype. (**c**) Absence of any changes in nerve conduction velocity (NCV) of the sciatic nerve. NCVs were recorded from 7 mice of each genotype at 3 to 4 months of age. (**d**) The distribution of axon diameters in nerves from 13-month-old mice were not different between mutant and wild type (WT) control mice (Kolmogorov-Smirnov two-sample test, p > 0.1). (**e**) The distribution of G-ratios (determined by dividing the inner (axonal) fiber diameter by the outer (axon plus myelin) fiber diameter) were also not different. (**f**) The relationships between axon diameter and the G-ratio were also not different, indicating that there was a normal relationship between myelin thickness and axon size in the mutant mice. N = 4 mutant mice at 3 WT littermate controls for the 13-month-old mice samples.
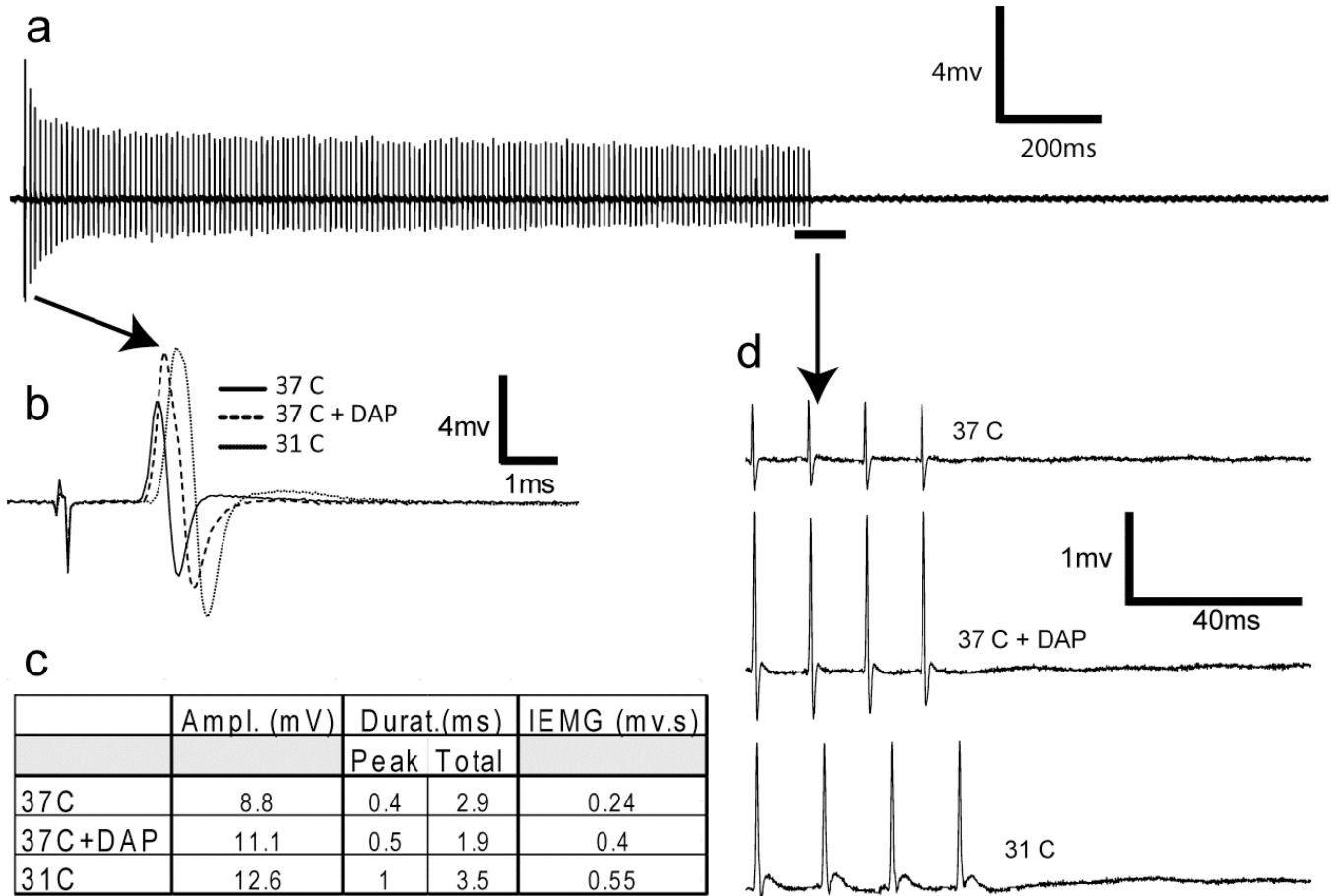
a

4mv

200ms

b

—— 37 C
---- 37 C + DAP
······ 31 C

4mv

1ms

d

37 C

1mv

40ms

37 C + DAP

31 C

c

	Ampl. (mV)	Durat.(ms)		IEMG (mv.s)
		Peak	Total	
37C	8.8	0.4	2.9	0.24
37C+DAP	11.1	0.5	1.9	0.4
31C	12.6	1	3.5	0.55

Figure 5.

Hint1 mutant mice do not show neuromyotonia. Representative results from a single 14-month-old mutant mouse in response to a 1.5-second, 100 Hz stimulus train are shown. (**a–d**) The complete record (**a**) was recorded at normal body temperature (37°C) and showed no evidence of neuromyotonia. The same stimulus protocol was repeated with body temperature lowered to 31°C and in the presence of 3,4 diaminopyridine ([3,4 DAP], 5 mg/kg), conditions that were sufficient to alter nerve conduction as shown by the first compound muscle action potential (CMAP) response under each condition (**b, c**). Neuromyotonia was not observed, either between pulses or after the entire stimulus train in any of the conditions used. (**d**) The final 4 CMAP responses from the 1.5-second, 100 Hz train from 37°C, 37° with 3,4 DAP, and at 31°C are shown with an expanded time scale.